

VARIATIONS IN THE ABUNDANCE OF TRANSIENTLY HEATED PARTICLES WITHIN  
NEARBY MOLECULAR CLOUDSF. BOULANGER,<sup>1,2</sup> E. FALGARONE,<sup>2,3</sup> J. L. PUGET,<sup>2</sup> AND G. HELOU<sup>1</sup>*Received 1989 December 6; accepted 1990 May 15*

## ABSTRACT

*IRAS* images of molecular clouds in the Chamaeleon, Taurus, and Ursa Major complexes show that the mid-IR emission from transiently heated particles is distributed very differently from the 100  $\mu\text{m}$  emission from large dust grains. The ratio between 12 and 100  $\mu\text{m}$  emission varies by more than one order of magnitude in each complex from  $\sim 5$  times to about one-quarter of the average value in the solar neighborhood. Within a complex, color variations are seen on all scales: between clouds a few pc in size and within these clouds on scales as small as a few tenths of a pc. No significant variations of the  $I_{\nu}(100 \mu\text{m})/A_{\nu}$  ratio are observed between clouds of widely different mid- to far-IR color. We show that neither the large amplitude of the color variations nor their morphology can be explained by changes of the excitation by the UV radiation field and conclude that the color variations trace variations in the abundance of transiently heated particles. We propose a scenario which relates the abundance variations to the cycling of interstellar matter between the gas-phase and grain surfaces. In this scenario small particles form in molecular clouds from molecules condensed on grains and photo-processed into organic mantles by UV light.

*Subject headings:* interstellar: abundances — interstellar: grains — interstellar: molecules

## I. INTRODUCTION

Near- and mid-infrared observations of the interstellar medium have revealed the existence of small particles with sizes intermediate between dust grains and the molecules identified through radio observations (Andriess 1978; Sellgren, Werner, and Dinerstein 1983; and review by Puget and Léger 1989). These particles are transiently heated to high temperatures each time they absorb a photon and cool by radiating in the near and mid-infrared. To account for the presence of the 3.3  $\mu\text{m}$  feature in the observations of Sellgren *et al.* (1983) Léger and Puget (1984) proposed that the small particles are polycyclic aromatic hydrocarbons (PAH). A population of small particles larger than the PAH, possibly small amorphous carbon grains, are also necessary to explain the emission observed at  $\lambda > 15 \mu\text{m}$  by *IRAS* (Desert, Boulanger, and Puget 1990, hereafter DBP). In the course of this paper we refer to the 12 and 25  $\mu\text{m}$  emitters, as small particles, without any assumption about their nature. Laboratory and astronomical data on small particles have been reviewed by Allamandola, Tielens, and Barker (1987), and Puget and Léger (1989). The small particles are an important constituent of the interstellar medium which accounts for  $\sim 40\%$  of the IR emission from the interstellar medium in the solar neighborhood (Boulanger *et al.* 1988) and contains  $\sim 30\%$  of the cosmic carbon if they are PAHs (Puget and Léger 1989). It has been suggested that small particles play an important role in the heating and the chemistry of interstellar gas (Omont 1986; d'Hendecourt and Léger 1987; Lepp and Dalgarno 1988*a, b*, Verstraete *et al.* 1990).

Each of the four *IRAS* wavelength bands samples the emission from a different type of particle (Puget *et al.* 1985; Draine and Anderson 1985; Chlewicki and Laureijs 1988; DBP). While the 100  $\mu\text{m}$  emission comes from large grains in equi-

librium with the radiation field, the 12 and 25  $\mu\text{m}$  emission, and, possibly, part of the 60  $\mu\text{m}$  emission is radiated by small particles with an increasing size for an increasing wavelength of emission. *IRAS* observations are thus an important source of information on the size spectrum and the composition of interstellar dust. With the purpose of characterizing the composition of dust away from strong sources of heating, *IRAS* observations have been used to measure IR colors for a large number of interstellar clouds heated by the general interstellar radiation field of the Galaxy (ISRF) (Boulanger, Baud, and Albada 1985; Leene 1986; de Vries and Le Poole 1985; Weiland *et al.* 1986; Boulanger and Pérault 1988; Heiles, Reach, and Koo 1988; Laureijs, Mattila, and Schnur 1987; Laureijs, Chlewicki, and Clark 1988; Beichman *et al.* 1988). Early in this series of studies it appeared that the ratio between mid-IR (12 and 25  $\mu\text{m}$ ) and 100  $\mu\text{m}$  emission varies widely from cloud to cloud. More recently Boulanger *et al.* (1989) and Puget (1989) reported color measurements for small areas,  $\sim 0.5$  pc in size, within fragments of moderate opacity ( $A_{\nu} < 2$  mag) in Taurus, Ophiuchus, Chamaeleon, and Ursa Major showing large variations in the color ratios  $R(12, 100) = I_{\nu}(12 \mu\text{m})/I_{\nu}(100 \mu\text{m})$  and  $R(25, 100) = I_{\nu}(25 \mu\text{m})/I_{\nu}(100 \mu\text{m})$  on all scales within the complexes down to that of the resolution of their measurements ( $I_{\nu}$  is the intensity at each wavelength in  $\text{MJy sr}^{-1}$ , without color correction). This result contrasts with the constancy of IR colors on scales  $\geq 1$  kpc observed in the Galaxy (Pérault, Boulanger, and Puget 1990) and the nearby galaxies M31 (Walterbos and Schwing 1987) and M33 (Rice *et al.* 1990).

The physical origin of the color variations seen in the nearby interstellar medium has not yet been elucidated. In their work Heiles, Reach, and Koo (1988) see a marginal dependence of  $R(12, 100)$  on gas velocity and provisionally conclude that small grains could be formed by shocks in the 10–20  $\text{km s}^{-1}$  velocity range and destroyed at higher velocities. Observations of limb-brightened profiles of the 12  $\mu\text{m}$  emission across B5 and a cloud in Chamaeleon led Beichman *et al.* (1988), Chlewicki and Laureijs (1988), and Laureijs *et al.* (1989) to propose

<sup>1</sup> Infrared Processing and Analysis Center, and Jet Propulsion Laboratory, California Institute of Technology.

<sup>2</sup> Radioastronomie, Ecole Normale Supérieure.

<sup>3</sup> Division of Physics, Mathematics and Astronomy, California Institute of Technology.

that color variations reflect excitation changes associated with the attenuation of the UV radiation field from the external to the inner parts of clouds. In this paper we bring further information on the nature of the color variations by presenting maps of IR colors for three nearby molecular complexes (§ II). These maps are used to establish various morphological and quantitative properties of the color variations (§ III). On the basis of these results and models of the transfer of UV photons in clouds we show that variations of the UV radiation field with opacity cannot explain the large amplitude of the color changes and conclude that the variations in the ratio between mid-IR and 100  $\mu\text{m}$  emission result from variations in the abundance of small particles (§ IV). In § V, we propose a scenario of the evolution of interstellar matter in molecular clouds which relates inhomogeneities in the abundance of small particles to the condensation and chemical processing of interstellar matter on grain surfaces and to turbulent motions in clouds. The main results of this work are summarized in § VI.

## II. OBSERVATIONS

We concentrate our study on three regions, Chamaeleon, Taurus, and Ursa Major, known to contain numerous molecular clouds located within 100–200 pc from the Sun. *IRAS* survey observations were co-added to produce  $9^\circ \times 9^\circ$  images of these three regions with 1' pixels and 4' spatial resolution. The selection of these fields was motivated by their position well outside the Galactic plane ( $|b| > 15^\circ$ ) which minimizes the risk of chance superposition between objects located at different distances along the line of sight and by their remoteness from any OB association. These two criteria ensure that clouds in each field are physically close to each other and are located in a rather homogeneous radiation field. The selected regions have been the target of extensive molecular observations. A complete CO map of the Taurus region with one-half degree resolution has been presented by Ungerechts and Thaddeus (1987). Higher resolution  $^{13}\text{CO}$  observations of Taurus have been obtained with the POM telescope of Bordeaux, France (Duvert, Cernicharo, and Baudry 1986; Cernicharo and Guélin 1987, Nercessian *et al.* 1988). Maps of the visual extinction in Taurus have been derived from star counts by Cernicharo, Bachiller, and Duvert (1985). An extensive CO survey of the Chamaeleon region with some  $^{13}\text{CO}$  observations was recently completed with the southern mini-telescope at Cerro-Tololo (Boulanger *et al.* 1990). Maps of the visual extinction in Chamaeleon have been presented by Gregorio-Hetem, Sanzovo, and Lépine (1988) and Laureijs *et al.* (1989). CO and H I maps of the high-latitude clouds in Ursa Major have been published by de Vries, Heithausen, and Thaddeus (1987). The Ursa clouds are part of an H I loop  $20^\circ$  long and  $2.5^\circ$  wide going through the Northern Celestial Pole (Heiles 1984).

The sensitivity of *IRAS* observations is sufficient to detect the emission of molecular clouds at all wavelengths over a wide range of colors. However, at 12 and 25  $\mu\text{m}$  the brightness of clouds is always smaller than a few percent of the zodiacal light and the accuracy on measurements of this brightness is generally limited by uncertainties on the zodiacal light subtraction. At longer wavelengths the uncertainties on the measurements come from the subtraction of emission from interstellar matter not associated with the clouds. Subtraction of foreground and background emission is particularly critical for this study because emission from nearby clouds extends over many degrees.

The Chamaeleon and Ursa Major fields are located at high

ecliptic latitudes ( $|\beta| > 30^\circ$ ). For these two fields a good subtraction of the zodiacal light and the background emission was obtained by fitting a plane over several positions around the clouds corresponding to minima of the 100  $\mu\text{m}$  emission. The Taurus field lies right in the ecliptic plane. This makes the subtraction of the zodiacal light somewhat more complex due to the zodiacal bands (Sykes 1988). These bands follow closely lines of constant ecliptic latitude. The two main bands lying in the vicinity of the ecliptic plane, the  $\alpha$  and  $\beta$  bands, have a brightness of  $\sim 0.6, 1.5, 0.6 \text{ MJy sr}^{-1}$  at 12, 25, and 60  $\mu\text{m}$ , respectively. To subtract the zodiacal light in this field we used regions of low 100  $\mu\text{m}$  emission to derive profiles (one per wavelength) of the zodiacal emission with ecliptic latitude. These profiles computed with  $1^\circ$  bins were linearly interpolated onto the initial grid which generated maps of the zodiacal emission with constant brightness along lines of constant  $\beta$ . After subtraction, the residual maps showed a gradient of zodiacal emission with ecliptic longitude. We subtracted this residual zodiacal emission by fitting a plane over the positions selected to measure the background emission. This subtraction was also necessary to subtract Galactic emission unrelated to the clouds. Due to the nonuniform distribution of background areas across the image, the profiles of zodiacal light were slightly distorted by the longitude gradient. The whole procedure was therefore repeated once more.

The accuracy of the subtraction of the zodiacal light and Galactic emission was assessed by measuring the scatter of the residual brightness in the regions selected for background fitting. For the Taurus field the uncertainty on the subtraction on the scale of the whole map is  $\sim 0.12, 0.20, 0.18, \text{ and } 0.6 \text{ MJy sr}^{-1}$  ( $1\sigma$ ). At 12 and 25  $\mu\text{m}$  these uncertainties are about two times smaller for the Chamaeleon field which is located close to the southern ecliptic pole. In the Taurus and Ursa Major complexes, uncertainties on the zero level on scales larger than a few degrees are about two times larger than on scales smaller than 1 degree. In Chamaeleon the images show no obvious large-scale changes of the zero level across the map.

False-color images of Chamaeleon and Taurus obtained from the 12, 60, and 100  $\mu\text{m}$  emission, mapped into blue, green, and red, respectively, are presented in Figure 1 (Plate 2). The striking color differences seen in these images correspond to dramatic changes in the spectrum of the IR emission from cloud to cloud and within clouds. To quantitatively study these color variations we made several cuts ( $\sim 8$ ) across each of the images. These cuts were used to obtain the IR brightness and colors for several tens of positions in each image. For illustration two cuts for each field are presented in Figure 2. The cuts shown in Figure 2 are indicated on the Chamaeleon and Taurus images in Figure 1. Before measuring the brightnesses we subtracted from each cut a linear baseline fitted over regions of low emission at all wavelengths. In all cases this subtraction represented a small correction to the background subtraction done on the images, and was within the large scale uncertainties quoted in the previous paragraph. In selecting the cuts we avoided regions locally heated by embedded stars so that all measurements relate to parts of the cloud heated from outside by the ISRF of the Galaxy.

The color measurements made on the cuts are presented in Figures 3–6. In Figure 3 the color ratio  $R(12, 100)$  is plotted against  $I_\nu(100 \mu\text{m})$ . Figure 4 presents  $R(12, 25)$  versus  $I_\nu(100 \mu\text{m})$ , Figure 5  $R(60, 100)$  versus  $I_\nu(100 \mu\text{m})$  and Figure 6  $R(12, 100)$  versus  $R(60, 100)$ . Measurements obtained in the different fields are plotted with different symbols. In Figures 3,

## PLATE 2

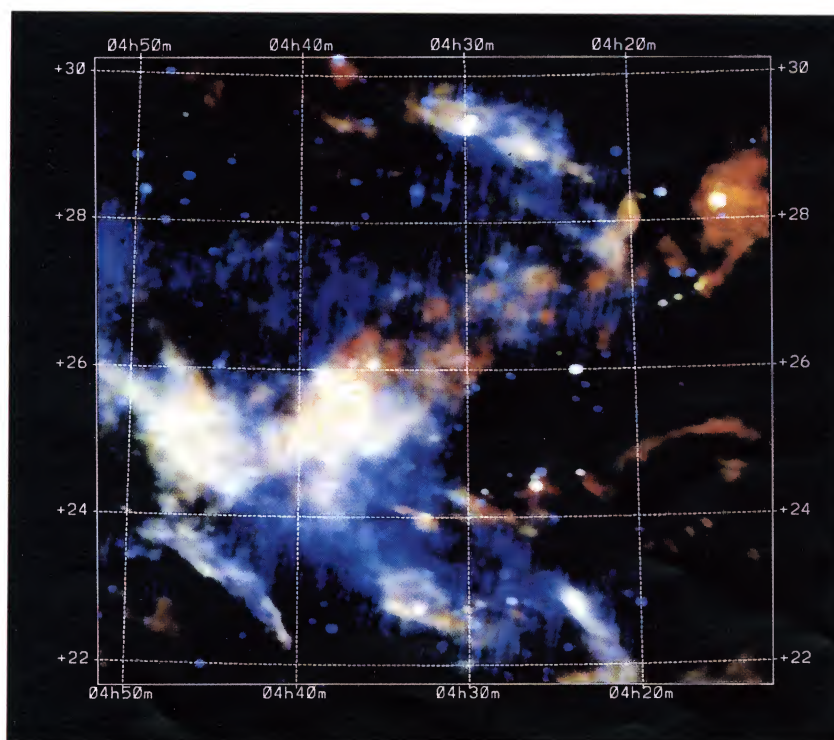
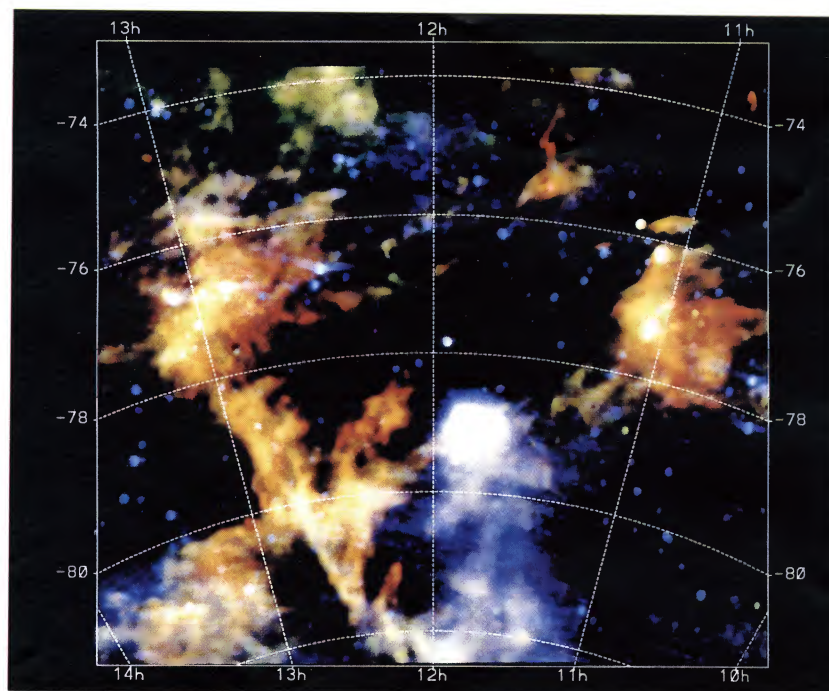


FIG. 1.—Color-coded image of the Chamaeleon (*top*) and Taurus (*bottom*) regions presenting a superposition of the 12, 60, and 100  $\mu\text{m}$  emission mapped into blue, green, and red, respectively. Note that different stretches were used to produce the two color plates. The difference is the strongest for the green. Clouds without 12  $\mu\text{m}$  emission and weak 60  $\mu\text{m}$  emission appear red in the Taurus plate and yellow in the Chamaeleon plate.

BOULANGER, FALGARONE, PUGET, AND HELOU (see 364, 137)

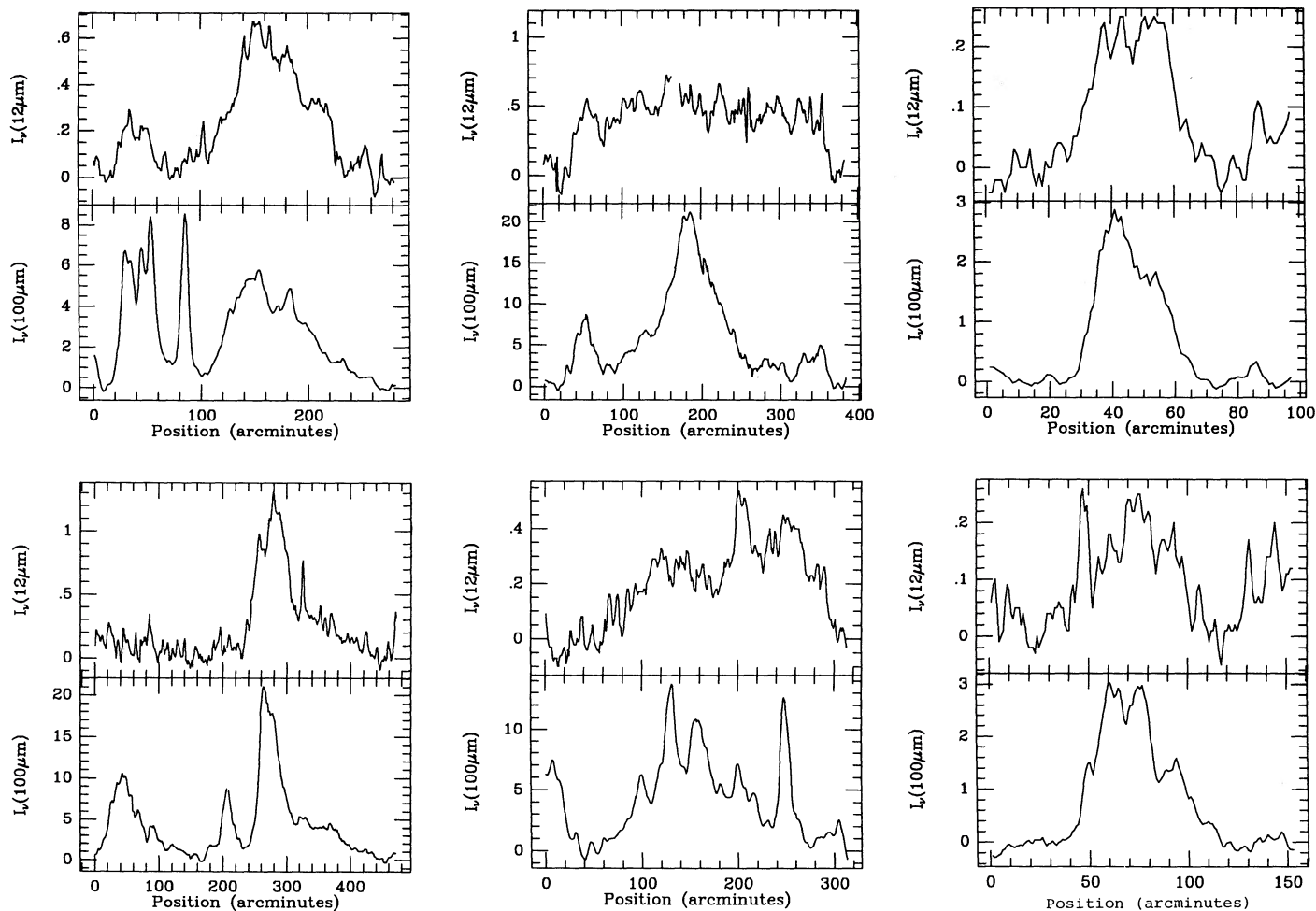


FIG. 2.—Examples of 12 and 100  $\mu\text{m}$  cuts across the Chamaeleon, Taurus, and Ursa Major images. In one of the Taurus cuts a few points were skipped at the position of a bright field star.

5, and 6 a few pairs of points are connected with dashed lines. These pairs represent color measurements at the same position for two different baselines: the global one defined for the whole cut and a local one defined for a specific structure within a cut. The  $R(12, 100)$  and  $R(60, 100)$  ratios are always smaller for the local baseline.

Numerous comparisons of  $I_v(100 \mu\text{m})$  with  $A_v$ ,  $^{13}\text{CO}$ , and CO for clouds in Chamaeleon, Taurus, and Ursa Major (Boulanger *et al.* 1990; Laureijs *et al.* 1989; Cernicharo and Guélin 1987; Snell, Heyer, and Schloerb 1989; de Vries, Heithausen, and Thaddeus 1987; Weikard and Duvert 1989), and in other clouds (see review by Boulanger 1989) have shown that the 100  $\mu\text{m}$  brightness is a good tracer of the column density of dust and gas up to  $A_v$  of about 2 mag. Measured slopes of the  $I_v(100 \mu\text{m})$  versus  $A_v$ , and  $I_v(100 \mu\text{m})$  versus  $W(^{13}\text{CO})$  correlations for molecular clouds with a total  $A_v$  of 2 to 5 mag are in the range 5 to 10 ( $\text{MJy sr}^{-1}$ )  $\text{mag}^{-1}$ . For atomic gas at high Galactic latitude, the correlation between IR and H I emission gives an average  $I_v(100 \mu\text{m})/N_{\text{H}}$  ratio of 0.85  $\text{MJy sr}^{-1}$  for  $10^{20} \text{ H cm}^{-2}$  (Boulanger and Pérault 1988) equivalent to a  $I_v(100 \mu\text{m})$  to  $A_v$  ratio of 16 ( $\text{MJy sr}^{-1}$ ) per mag for the standard  $A_v/N_{\text{H}}$  ratio of  $5.3 \times 10^{-22} \text{ mag cm}^2$ . These values may be used to convert the 100  $\mu\text{m}$  brightnesses in Figures 3 and 5 into  $A_v$  or  $N_{\text{H}}$ . Most of the measurements presented in these figures correspond to lines of sight with  $A_v < 2$  mag.

### III. OBSERVATIONAL PROPERTIES

#### a) Average Colors

Average colors were obtained for each field by integrating the emission of all the clouds present in the images. These average colors are given in Table 1. Uncertainties on these numbers result from uncertainties on the background level. In Chamaeleon, clouds with very distinct colors are seen spatially separated from each other in Plate 2. This favorable arrangement enabled us to measure an average color for each cloud (Table 1). The round cloud at ( $\alpha \sim 12 \text{ hr}$ ,  $\delta$  about  $-79^\circ$ ) close to the center of the image (with the tail to the south and the bridge toward Cha I ( $\alpha \sim 11^{\text{h}}10^{\text{m}}$ ,  $\delta \sim -77^\circ$ ) to the west) accounts for all the mid-IR emission of the complex but only one-third of the 100  $\mu\text{m}$  emission. The two other main clouds in the complex, Cha I and Cha II to the east and the west of the plate show no or little 12  $\mu\text{m}$  emission. The color stretch used to display the Taurus images (Plate 2) was different from those used for Chamaeleon, in particular for the green color (60  $\mu\text{m}$ ). Clouds without 12  $\mu\text{m}$  emission appear deep red in the Taurus plate while they are yellow in the Chamaeleon plate. In Taurus most of the 12 and 25  $\mu\text{m}$  emission comes from an extended halo, several degrees in size, seen projected against regions with weak or no mid-IR emission (see Plate 2 and cuts in Fig. 2). The halo envelops entirely Heiles Cloud 2 ( $\alpha \sim 4^{\text{h}}38^{\text{m}}$ ,  $\delta \sim 25^\circ30'$ ). The cut across this cloud presented in

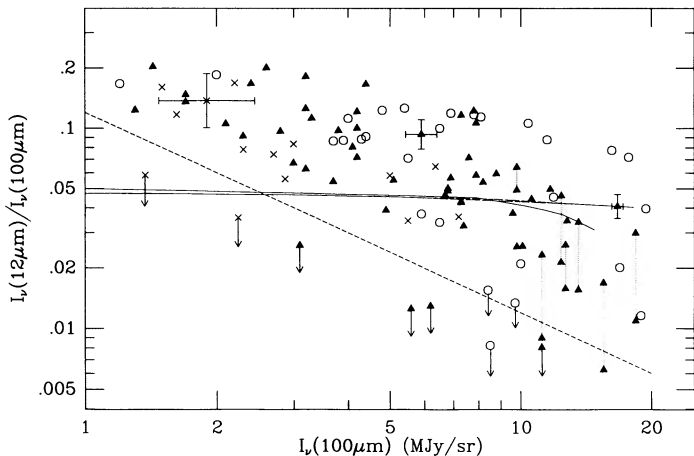


FIG. 3.—Plot of the color ratio  $R(12, 100) = I_v(12 \mu\text{m})/I_v(100 \mu\text{m})$  vs.  $I_v(100 \mu\text{m})$ . The symbols are circles for Chamaeleon, solid triangles for Taurus, and crosses for Ursa Major. The dashed line shows the sensitivity limit for measurements of the  $12 \mu\text{m}$  brightness. All data points near this line are upper limits on  $R(12, 100)$ . For a few positions we measured the colors for two different baselines: the global one defined for the whole cut and one defined locally from local minima of emission near the position of the measurements. The corresponding pairs of data points are connected by a dotted line.  $R(12, 100)$  is always smaller for the local baseline. To keep the plot clear error bars are only given for three data points selected as representative of points with low, average, and high  $I_v(100 \mu\text{m})$ . The solid line represents a model calculation by Chlewicki and Laureijs (1988) for a uniform density and a total  $A_v$  of 2 mag. This line has been normalized to a  $R(12, 100)$  value of 0.05 at small  $I_v(100 \mu\text{m})$  to fit with the average colors of cirrus (see Table 1). Two dashed lines illustrate calculations by Bernard *et al.* (1990) for a  $1/r^2$  density profile and a total  $A_v$  of 2 and 4 mag. These two lines overlap over most of their length.

Figure 2 shows a strong  $12 \mu\text{m}$  emission from the halo and no  $12 \mu\text{m}$  emission from the denser part of the cloud detected in  $^{13}\text{CO}$ . From Heiles Cloud 2, the blue halo in Plate 2 extends to the south-west toward L1529 ( $\alpha \sim 4^{\text{h}}30^{\text{m}}$ ,  $\delta \sim 24^{\circ}20'$ ) and to the north-west toward L1495 ( $\alpha \sim 4^{\text{h}}15^{\text{m}}$ ,  $\delta \sim 28^{\circ}$ ). The geometry makes it difficult to separate the contributions of the halo and of the denser parts of the clouds to the  $100 \mu\text{m}$  emission of the complex. In Ursa Major, over most of the surface of the clouds, the colors are uniform within a factor of 2. We observe in this field no regions without mid-IR emission.

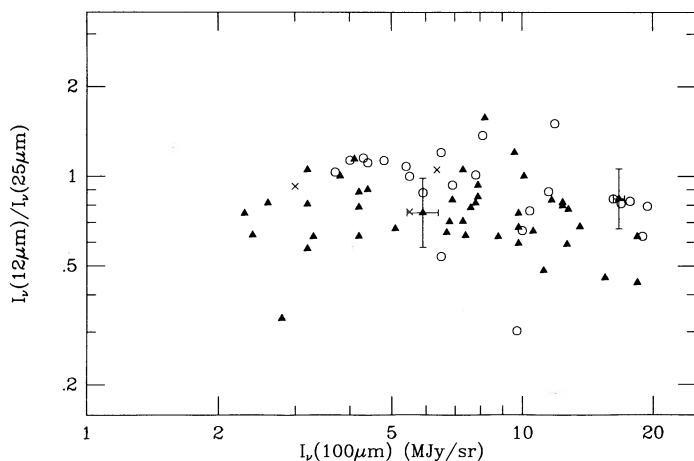


FIG. 4.—Plot of  $R(12, 25)$  vs.  $I_v(100 \mu\text{m})$ . Only data points with  $I_v(25 \mu\text{m}) > 0.25 \text{ MJy sr}^{-1}$  are included. Error bars are given for the same points as in Fig. 3. Points with upper limits at 12 and 25  $\mu\text{m}$  do not appear on this plot.

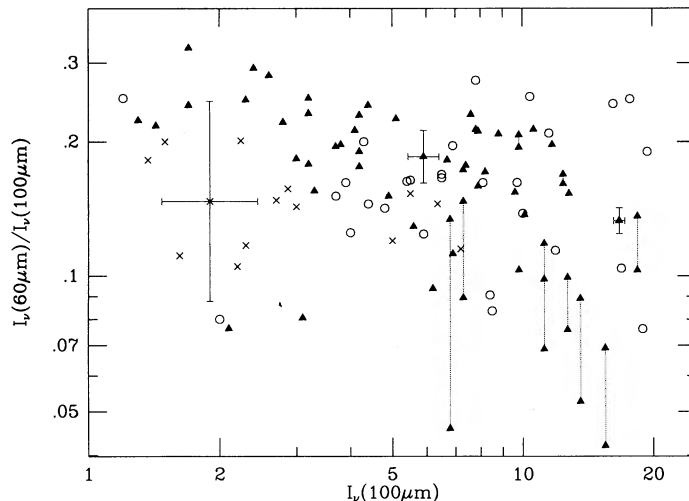


FIG. 5.—Plot of  $R(60, 100)$  vs.  $I_v(100 \mu\text{m})$ . Measurements obtained at the same position for two different baselines (see Fig. 3) are connected by a dotted line. Error bars are given for the same data points as in Fig. 3.

However, values of  $R(12, 100)$  several times greater than the average value for the whole cloud, and comparable to the maximum values seen in the two other clouds, are measured along narrow filaments at the edge of the clouds (see cuts in Fig. 2).

It is remarkable that for all three complexes the average  $R(12, 100)$  and  $R(25, 100)$  colors listed in Table 1 coincide within the uncertainties with the average colors of the solar neighborhood although these colors vary by an order of magnitude from place to place within each complex. This result has no straightforward interpretation. It does not necessarily mean that the average abundance of small particles in molecular clouds is the same as in the atomic interstellar medium because a large fraction of the small particles in molecular clouds could be condensed on grains and not seen in emission (§ V). The  $R(60, 100)$  color, 0.14 for the three complexes, is significantly smaller than the value of 0.21 for the solar neighborhood. The comparison between the slope of the  $I_v(100 \mu\text{m})$ — $A_v$  relation in molecular clouds and its slope in atomic gas indicates that the radiation field is higher by a factor 2 to 3 in the atomic

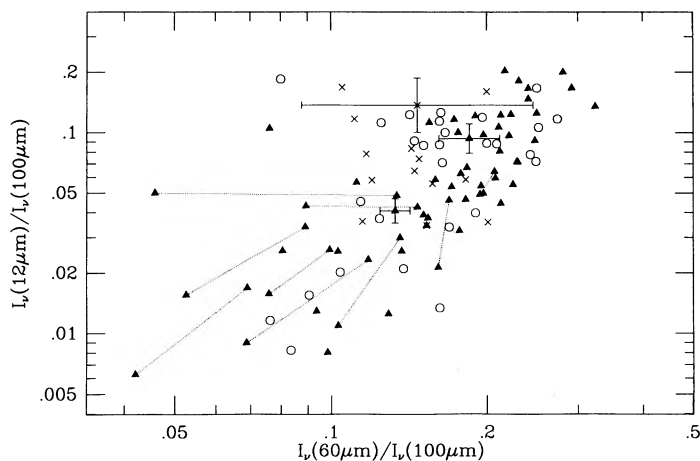


FIG. 6.—Plot of  $R(12, 100)$  vs.  $R(60, 100)$ . Measurements obtained at the same position for two different baselines (see Fig. 3) are connected by a dotted line. Error bars are given for the same data points as in Fig. 3.

TABLE 1  
AVERAGE COLORS OF CLOUDS

Name <sup>a</sup>	$R(12, 100)$	$R(25, 100)$	$R(60, 100)$	$I_{\nu}(100 \mu\text{m})/A_{\nu}$ (MJy sr <sup>-1</sup> ) per mag <sup>b</sup>
Chamaeleon .....	0.038 ± 0.015	0.044 ± 0.02	0.145 ± 0.02	
Cha I .....	<0.01	<0.02	0.15 ± 0.02	6.5 ± 1.
Cha II .....	<0.013	<0.025	0.11 ± 0.02	7.0 ± 1.
Cha Round .....	0.094 ± 0.01	0.103 ± 0.01	0.21 ± 0.01	10.5 ± 1.
Tail .....	0.12 ± 0.03	0.094 ± 0.03	0.16 ± 0.02	
Bridge .....	0.067 ± 0.015	0.071 ± 0.015	0.18 ± 0.02	
Taurus .....	0.043 ± 0.015	0.050 ± 0.02	0.14 ± 0.02	
Ursa .....	0.048 ± 0.015	0.052 ± 0.02	0.14 ± 0.02	
Solar Neighborhood .....	0.042 ± 0.012	0.054 ± 0.016	0.21 ± 0.01	16. ± 1.

<sup>a</sup> For Chamaeleon we give the average colors for the whole complex and for subregions spatially separated from each other. Cha I is the western cloud, Cha II the eastern cloud, Cha Round the bright round cloud located close to the center of the plate, Tail the southern extension of Cha Round, and Bridge the low brightness bridge seen between Cha Round and Cha I (see Pl. 2). The average colors for the solar neighborhood (Boulanger and Pérault 1988) are given for comparison.

<sup>b</sup> Numbers from Laureijs *et al.* 1989; Boulanger *et al.* 1990.

interstellar medium compared to regions of molecular clouds which radiate the bulk of the 100  $\mu\text{m}$  emission (Boulanger 1989). If all of the 60 and 100  $\mu\text{m}$  emission were coming from large dust grains the decrease in equilibrium temperature associated with the attenuation of the radiation field,  $\sim 15\%$ , would account for the difference in  $R(60, 100)$  color. However, across the Galaxy and the nearby galaxies M31 and M33 the  $R(60, 100)$  color of cirrus is observed to be only weakly dependent on the intensity of the ISRF. This has been interpreted as evidence for a significant contribution of small, transiently heated particles to the 60  $\mu\text{m}$  emission (Walterbos and Schwing 1987). Thus the difference in  $R(60, 100)$  between atomic gas and molecular clouds may not result entirely from a temperature decrease of large grains. It could be indicative of a change in the contribution of small particles to the 60  $\mu\text{m}$  emission, or in the optical properties of large grains. In the model of DBP for the average ISRF in the solar neighborhood the very small grains contribute 60% of the 60  $\mu\text{m}$  emission.

#### b) Color Variations

The plot of  $R(12, 100)$  versus  $I_{\nu}(100 \mu\text{m})$  in Figure 3 reveals three important features: (1) a systematic decrease of  $R(12, 100)$  with increasing  $I_{\nu}(100 \mu\text{m})$  (close to a  $1/I_{\nu}(100 \mu\text{m})$  law), (2) a scatter around this systematic trend of almost a factor of 10 in  $R(12, 100)$  at all  $I_{\nu}(100 \mu\text{m})$ , (3) the occurrence of the largest values of  $R(12, 100)$  only at low  $I_{\nu}(100 \mu\text{m})$ , while lines of sights without any measurable 12  $\mu\text{m}$  emission are seen for all values of  $I_{\nu}(100 \mu\text{m})$ . The median value of  $R(12, 100)$  decreases from 0.14 for  $I_{\nu}(100 \mu\text{m}) \sim 2$  MJy sr<sup>-1</sup>, to 0.07 at  $I_{\nu}(100 \mu\text{m}) \sim 5$  MJy sr<sup>-1</sup>, and 0.03 for  $I_{\nu}(100 \mu\text{m})$  between 10 and 20 MJy sr<sup>-1</sup>. For  $I_{\nu}(100 \mu\text{m}) < 5$  MJy sr<sup>-1</sup>, measured values of  $R(12, 100)$  range from values  $\leq 0.03$  up to 0.2. At higher  $I_{\nu}(100 \mu\text{m})$  the scatter is as large. The largest values of  $R(12, 100)$  do not exceed 0.12 but smaller upper limits are obtained. In each field the largest values of  $R(12, 100)$  are a factor of 5 higher than the average color ratio for the solar neighborhood, 0.042 (Boulanger and Pérault 1988). The lowest values of  $R(12, 100)$  are upper limits which are a factor of 4 smaller than this average value. Note that for  $R(12, 100) > 0.08$  small particles radiate more power in the mid-IR than large grains in the far-IR.

Cuts in Figure 2 show that the high  $R(12, 100)$  values at low  $I_{\nu}(100 \mu\text{m})$  do not result from larger uncertainties on the color ratios for low  $I_{\nu}(100 \mu\text{m})$ . They also illustrate the variety of

morphologies of regions of high  $R(12, 100)$ . The linear projected size of these regions varies from 0.3 pc to 10 pc. More examples have been presented by Boulanger (1989) and Puget (1989). Where  $R(12, 100) > 0.12$  the 100  $\mu\text{m}$  brightness is always smaller than  $\sim 6$  MJy sr<sup>-1</sup> which corresponds to a column density smaller than  $\sim 10^{21}$  H cm<sup>-2</sup>. The physical connection between these regions and regions of higher  $I_{\nu}(100 \mu\text{m})$  and lower  $R(12, 100)$  is not obvious. In Taurus regions of high  $R(12, 100)$  seem to surround regions of low  $R(12, 100)$  and higher  $I_{\nu}(100 \mu\text{m})$ , but in Chamaeleon the two types of regions appear spatially separated from each other. In both regions several clouds show a systematic decrease of  $R(12, 100)$  from the edge to the center (see cuts in Fig. 2 and also Laureijs *et al.* 1989; Beichman *et al.* 1988). However, several clouds or fragments of clouds in Chamaeleon (Cha I and Cha II) and Taurus (the cloud at the top right corner of Plate 2: L1495 at  $\alpha \sim 4^{\text{h}}15^{\text{m}}$ ,  $\delta \sim 28^{\circ}$ , and L1506 the filament on the right-hand side of the plate at  $\alpha \sim 4^{\text{h}}18^{\text{m}}$ ,  $\delta \sim 25^{\circ}$ ) with little or no 12  $\mu\text{m}$  emission are not surrounded by regions of high  $R(12, 100)$ .

In Figure 4 we show the distribution of  $R(12, 25)$  versus  $I_{\nu}(100 \mu\text{m})$ . Compared to the  $R(12, 100)$  ratio,  $R(12, 25)$  appears relatively constant from cloud to cloud and, unlike  $R(12, 100)$ , it does not show any dependence on  $I_{\nu}(100 \mu\text{m})$ . If we take into account the uncertainties on the measurements the real scatter of  $R(12, 25)$  is about a factor of 2, one order of magnitude smaller than that observed for  $R(12, 100)$ . This result suggests a close correlation between the populations of particles generating the 12 and 25  $\mu\text{m}$  emission. This is not a trivial constraint since detailed dust models predict that only about one-half of the 25  $\mu\text{m}$  emission is coming from the particles giving rise to the 12  $\mu\text{m}$  emission (Chlewicki and Laureijs 1988; DBP).

The  $R(60, 100)$  color (Figs. 5–6) shows considerable scatter, comparable to that observed for  $R(12, 100)$ .  $R(60, 100)$  is observed to vary from  $\sim 0.05$  to 0.3. Figure 5 does not show any clear relation between  $R(60, 100)$  and  $I_{\nu}(100 \mu\text{m})$ . For Taurus  $R(60, 100)$  colors are globally seen to decrease with increasing  $I_{\nu}(100 \mu\text{m})$  but data for Chamaeleon and Ursa Major do not show this trend. A color decrease similar to the one seen for our Taurus data was found for B5 in Perseus by Langer *et al.* (1989), and for Heiles 2 and B18 in Taurus by Snell, Heyer, and Schloerb (1989). For one cloud in Chamaeleon and three high-latitude clouds, Laureijs, Chlewicki and Clark (1988) reported the reverse effect, an increase of  $R(60, 100)$  with  $I_{\nu}(100 \mu\text{m})$ . In Figure 6 among the Taurus data

points there is a good correlation between  $R(12, 100)$  and  $R(60, 100)$  but this correlation is not as obvious in Chamaeleon and is not seen at all in Ursa Major where  $R(60, 100)$  shows little variation.

For large grains in thermal equilibrium the total amplitude of the  $R(60, 100)$  variations corresponds to a change in the intensity of the radiation field by a factor of 20 (DBP). Since the intensity of the radiation field is rather constant over the regions we are studying (see § II) variations of  $R(60, 100)$  cannot be fully attributed to changes in the intensity of the ISRF. If the scatter in  $R(60, 100)$  is due to the contribution of small particles to the  $60 \mu\text{m}$  emission (Draine and Anderson 1985; Chlewicki and Laureijs 1988; DBP), the lack of clear correlation between  $R(12, 100)$  and  $R(60, 100)$  suggests that small particles emitting at  $60 \mu\text{m}$  are not closely related to those emitting at  $12 \mu\text{m}$ . An alternative explanation for the scatter in  $R(60, 100)$  is that the optical properties of large grains change from place to place in clouds. Such changes could be related to the formation of mantles (§ V). Note that the color variations discussed here have different characteristics from those seen in the vicinity of hot stars and between galaxies (Helou 1986; Ryter, Puget, and Pérault 1987; Boulanger *et al.* 1988) which are the combined effect of warming of large dust grains and of destruction of small particles emitting at  $12 \mu\text{m}$ .

#### IV. EXCITATION EFFECTS

##### a) Ultraviolet Photons

The small particles which have been proposed to account for the near and mid-IR emission from the interstellar medium absorb mostly in the ultraviolet (UV, see Puget and Léger 1989). The variations of the mid-IR to far-IR emission ratio could thus result from changes in the rate of excitation of the small particles due to anisotropy and intensity variations in the UV radiation field. This idea was put forward by Beichman *et al.* (1988), Chlewicki and Laureijs (1988), and Laureijs *et al.* (1989) to account for the limb brightening of the  $12 \mu\text{m}$  emission seen across several clouds (§ III). Models to test quantitatively this idea have been presented by these authors and DBP. Results of these models are presented in Figure 3 for three cases. The first is a calculation by Chlewicki and Laureijs (1988) for a uniform spherical cloud of total  $A_v = 2$  mag, the second and third are from calculations using DBP's dust model for clouds with a total  $A_v$  of 2 and 4 mag and a  $1/r^2$  density profile (Bernard *et al.* 1990). These calculations are based on two independent but rather similar dust models. In both cases the  $12 \mu\text{m}$  emission is attributed to PAHs, the absorption cross sections of which are taken from the laboratory measurements reported by Léger, d'Hendecourt, and Défourneau (1989). Most of the excitation of PAHs comes from UV photons, which is the most favorable case to account for the limb brightening of the  $12 \mu\text{m}$  emission because it is this part of the radiation field which is the most efficiently attenuated in clouds.

The models are only indicative in the sense that the variation of the radiation field across a cloud depends not only on its overall opacity but also on its density structure and geometry (Boissé 1990). If most of the mass in the clouds is in clumps with sizes smaller than a few arcminutes the effective extinction may be higher than the one derived from star counts and the IRAS  $100 \mu\text{m}$  data. Nevertheless, the large disagreement between the data and model calculations, even for  $A_v$  as large as 4 mag, shows that the decrease of the UV radiation field

with optical depth from the surface is quantitatively unable to explain the systematic decrease of  $R(12, 100)$  with increasing  $I_v(100 \mu\text{m})$ . For the uniform density case  $R(12, 100)$  decreases by 40% from the edge of the cloud to the line of sight through its center where  $I_v(100 \mu\text{m}) \sim 15 \text{ MJy sr}^{-1}$ , while we observe a systematic decrease of a factor 5 over the same range of  $I_v(100 \mu\text{m})$ . For the model of Bernard *et al.* the predicted effect is even smaller. The difference between the two models comes mostly from different assumptions regarding absorption properties of large grains. In their calculation of Chlewicki and Laureijs assume that large grains absorb a large fraction of their energy in the red due to the formation of mantles. This assumption enhances the effect of the attenuation of the UV field on the  $R(12, 100)$  color. In all of the models the change in  $R(12, 100)$  is small because the attenuation of the radiation field reduces the 12 and  $100 \mu\text{m}$  emission at roughly the same rate. Large grains which emit at  $100 \mu\text{m}$  absorb over the whole ISRF spectrum. Attenuation of the UV part of the radiation field reduces the heating of these grains and consequently their bolometric emission and temperature. Due to the temperature decrease, the dust emission shifts towards longer wavelengths which makes the decrease of  $100 \mu\text{m}$  emission faster than that of the dust heating. This reduction of the  $100 \mu\text{m}$  emission predicted by the model is verified by observations. It corresponds to the reduction by a factor 2 to 3 observed in the  $I_v(100 \mu\text{m})/A_v$  ratio between atomic gas and molecular clouds (Boulanger 1989). The models which fail to explain the limb brightening of the  $12 \mu\text{m}$  emission do reproduce the observed decrease in the slope of the  $100 \mu\text{m}$  versus  $A_v$  relation from atomic gas to molecular clouds (Chlewicki and Laureijs 1988; Bernard *et al.* 1990).

Changes in the rate of UV excitation of the small particles are also inadequate to explain the scatter observed in Figure 3 at a given  $I_v(100 \mu\text{m})$ . Again, to increase or decrease the  $R(12, 100)$  color of a cloud of a given opacity by some factor the UV radiation field at its surface must be increased or decreased by a much larger factor because large grains emitting at  $100 \mu\text{m}$  also absorb in the UV. For example, in the calculations of Laureijs (1989) and DBP it is necessary to scale the UV part of the ISRF by a factor of  $\sim 5$  to increase  $R(12, 100)$  by only 50%. Such a change of the radiation field implies an increase of the  $100 \mu\text{m}$  emissivity per dust grain measured by the ratio  $I_v(100 \mu\text{m})/A_v$  by a factor of  $\sim 3$ . The interpretation of the scatter in  $R(12, 100)$  at a given  $I_v(100 \mu\text{m})$  in Figure 3 along this line would imply that the radiation field at the surface of the clouds varies by more than one order of magnitude from cloud to cloud. Such large inhomogeneities in the UV radiation field are completely excluded for the Chamaeleon, Taurus, and Ursa Major complexes which are located far-away from any OB association. While shadow effects between clouds can attenuate the radiation field and create regions of low  $R(12, 100)$ , the high values of  $R(12, 100)$  would require UV radiation fields an order of magnitude more intense than the average ISRF, which cannot be obtained without nearby O or early B stars. Furthermore, such an interpretation would imply variations of  $I_v(100 \mu\text{m})/A_v$  by an order of magnitude correlated with those of  $R(12, 100)$ , which are excluded by the results of the comparison between  $A_v$  and  $I_v(100 \mu\text{m})$  in Chamaeleon (see Table 1). Therefore, it is clear that the main observational properties of the variations of  $R(12, 100)$  established in § III, namely their systematic decrease with increasing  $I_v(100 \mu\text{m})$ , and the large scatter observed for all values of  $I_v(100 \mu\text{m})$  cannot be quantitatively explained by variations in the excitation of the small particles by UV photons.

### b) Other Mechanisms

An alternative explanation of the color variations could be the existence of an additional source of excitation of the small particles other than star light in the regions of high  $R(12, 100)$  and  $R(25, 100)$ . For the three complexes the emission from small particles at  $\lambda < 25 \mu\text{m}$  is on average  $\sim 10^{-31}$  W per hydrogen atom, which represents  $\sim 25\%$  of the total power radiated by the clouds in the infrared and sub-millimeter. It is difficult to imagine a source of energy other than starlight which could contribute any significant fraction of this emission. For example the energy per nucleon associated with turbulent motions for a cloud of size  $D$ , using the line width-size relation  $\Delta V(\text{FWHM}) = (D/10 \text{ pc})^{0.5} \text{ km s}^{-1}$ , is  $E_c = 3/2\sigma_v^2 = 3 \times 10^{-21}(D/10 \text{ pc})\text{J/H}$ . If shocks associated with turbulent motions in clouds were at the origin of the emission from small particles the turbulent energy would be dissipated in  $\sim 10^3$  yr. Since molecular clouds are observed to be in virial equilibrium the gravitational energy is of the same order of magnitude as the turbulent energy and is not a potential energy source either. The heating rate of gas by photo-electrons from grains or large molecules is  $\sim$  a few  $10^{-33}$  W/H at the surface of molecular clouds and smaller inside clouds (Lepp and Dalgarno 1988b; Verstraete *et al.* 1990). If the high values of  $R(12, 100)$  were the result of collisional excitation of PAHs, the gas cooling rate would be about two orders of magnitude higher than the photo-electric heating and an additional heating mechanism of the gas would need to be found. It is also unclear how collisional excitation would explain the color variations seen on small scales inside clouds.

## V. ABUNDANCE EFFECTS

### a) Potential Explanation

In view of the results of § IV, namely the inability of UV excitation to account for the variations of colors and the difficulty in finding any alternative source of excitation of small particles, we conclude that changes in the  $R(12, 100)$  and  $R(25, 100)$  colors reflect changes in the abundance of small particles. Once this conclusion is accepted the observations give us three clues. (1) The existence of  $R(12, 100)$  and  $R(25, 100)$  colors several times higher than the average color in the atomic medium suggests that PAHs or some other family of particles emitting in the mid-IR are generated in molecular clouds. (2) The strong limb brightening seen in many clouds and the systematic decrease of the median value of  $R(12, 100)$  with  $I_\nu(100 \mu\text{m})$  indicate that UV photons are involved not only in the excitation of the small particles but also in their generation as proposed by Duley (1989). (3) The fact that at a given  $I_\nu(100 \mu\text{m})$  observed colors vary by about one order of magnitude tells us that the abundance of small particles is a function of some additional parameter besides the UV field and the gas column density. We propose that this additional parameter is the *recent history* of the matter. On the basis of the clues given by the data and this hypothesis we propose a scenario which relates color variations to the cycling of interstellar matter between the gas and grain surfaces. In this scenario small particles form in molecular clouds from molecules condensed on grains and photo-processed into organic mantles by UV light. Regions of low  $R(12, 100)$  correspond to pieces of clouds where small particles are condensed onto grains and do not form, while high values of  $R(12, 100)$  are found where small particles are formed and detached from grain mantles by UV photons, through photo-desorption (Draine and Salpeter 1979) or as a

result of localized heating (Duley 1989). Turbulent motions in clouds play a key role in this scenario. Through transient compression of the gas they create the dense regions where condensation of molecules on grains can happen. In addition, by bringing together pieces of cloud with different recent histories, they cause the color inhomogeneities seen on small scales. In the following two subsections we describe the significant steps and aspects of this scenario in more detail. In the last subsection we propose some observational tests.

### b) Elementary Cycle on Grains

The cycling of interstellar elements between the gas phase and grain surfaces and supporting evidence from laboratory experiments and observations have been extensively described by Greenberg (1982). We outline here the significant parts of this cycle. The condensation of molecular ices on dust grains in dark clouds is demonstrated by observations of infrared absorption bands such as the recent survey of the  $3.1 \mu\text{m}$  feature of  $\text{H}_2\text{O}$  ice in Taurus which indicates that water is condensed on grains for all lines of sight with  $A_v > 3$  mag (Whittet *et al.* 1988) and within the present uncertainties on the data for none of the lines of sight with smaller  $A_v$ . The shape of this feature cannot be explained by  $\text{H}_2\text{O}$  alone and probably results from an amorphous mixture of water with other molecules (Smith, Sellgren, and Tokunaga 1989). Laboratory experiments have shown that processing by UV photons transforms volatile molecular ices into refractory mantles made of large organic molecules. The existence of these organic mantles even in envelopes of molecular clouds is supported by the observation of the aliphatic C-H stretching mode at  $3.4 \mu\text{m}$  in absorption along lines of sight which lack the  $\text{H}_2\text{O}$   $3.1 \mu\text{m}$  feature such as towards the source IRS7 in the Galactic center (Allen and Wickramasinghe 1981; Butchart *et al.* 1986).

These mantles are a big reservoir of hydrocarbons and could be the source of the small particles seen in emission at 12 and  $25 \mu\text{m}$  provided that organic molecules or aggregates of molecules are released to the gas phase with a sufficient efficiency when mantles are exposed to UV photons. To explain the limb brightening of  $R(12, 100)$  and  $R(25, 100)$  the detachment process must happen preferentially at the edge of clouds. Mechanisms directly related to the absorption of a UV photon such as photo-desorption and detachment during localized heating fulfill this condition. However, these two mechanisms should more effectively detach individual molecules than large aggregates which seems to contradict the good correlation between enhancements in 12 and  $25 \mu\text{m}$  emission, the latter expected to come from larger particles than the former. Explosion of grain mantles triggered by the energy released in a chain of chemical reactions is also a plausible detachment process. Such an explosion will happen if a grain covered with active radicals is heated above a threshold temperature  $\sim 27$  K (d'Hendecourt *et al.* 1982). Absorption of a UV photon inducing a transient and localized heating of the grain above the threshold temperature may be sufficient to trigger the explosion.

Grain heating at the edges of clouds should also liberate small particles trapped into the volatile part of the grain mantles. The small particles detached from grains are probably a complex mixture of different types of hydrocarbons and carbon aggregates. The absence of the  $3.3 \mu\text{m}$  aromatic feature in the absorption spectra with the  $3.4 \mu\text{m}$  aliphatic feature suggests that PAHs are not the dominant type of molecules on

grain mantles. However, PAHs known to be more resistant to thermo-dissociation than other hydrocarbons could become the dominant species after a sufficiently long exposure of matter to the unattenuated ISRF. Further, the strong heating associated with photon absorption could lead to the conversion of aliphatic hydrocarbons to PAHs as suggested by the experiments of Sakata and Wada (1989) on quenched carbonaceous composites.

Puget and Léger (1989) estimated that on average in the atomic interstellar medium  $\sim 17\%$  of the carbon is in PAHs. In the molecular complexes we have studied we find color ratios,  $R(12, 100)$ , varying by more than one order of magnitude around the average value in the solar neighborhood. To account for the color variations, the carbon abundance in small particles in the gas phase must vary from less than  $\sim 5\%$  to more than half of the cosmic abundance. For our explanation to the color variations to hold, an important fraction of the cosmic carbon ( $\sim 50\%$ ) must cycle between the gas phase and dust mantles. From the strength of the  $3.4 \mu\text{m}$  feature in the direction of the Galactic center Tielens and Allamandola (1987) estimate that  $25\%–50\%$  of the carbon along this line of sight is in organic mantles. There is thus a reasonable agreement between the quantity of carbon observed to be in mantles and the amplitude of cycling necessary to account for the color variations.

### c) Elementary Cycle in Clouds

The condensation of gas species onto dust grains requires the existence in molecular clouds of regions which remain sufficiently dense over a sufficient span of time. For light molecules the condensation time scale, assuming a sticking probability of one, is (Draine 1985):

$$\tau_{\text{con}} = 3 \times 10^5 \text{ yr} \left( \frac{n_{\text{H}_2}}{5 \times 10^3 \text{ cm}^{-3}} \right)^{-1} \sum_{21}^{-1} \times \left( \frac{\mu}{20 m_{\text{H}}} \right)^{1/2} \left( \frac{T}{20 \text{ K}} \right)^{-1/2}, \quad (1)$$

where  $\mu$  is the molecular weight of the molecules and  $\sum_{21}$  the total grain cross-section expressed in  $10^{-21} \text{ cm}^2$  per hydrogen atom. The condensation time scale for large molecules such as PAHs depends on their relative velocity with respect to dust grains. For a relative velocity assumed to be  $\sim$  a few  $10^3 \text{ cm s}^{-1}$  (see Omont 1986) the time scale for condensation of PAHs is about an order of magnitude higher than that of small molecules. The normalized cross section  $\sum_{21}$  is  $\sim 1$  for the size distribution of spherical grains proposed by Mathis, Rumpl, and Nordsieck (1977) but if interstellar grains are fractal in nature the total grain surface could be higher than this value by as much as an order of magnitude (Meakin and Donn 1988) which will lower the condensation time scale accordingly, at least for small molecules. For large molecules the reduction of the time scale is not as straightforward because their relative velocity with respect to grains will be reduced as the cross section of grains increases.

Observations at high-angular resolution in several transitions of CO and isotopic variants, and in the  $J = 2-1$  transition of CS (Falgarone and Péroult 1988; Falgarone, Phillips, and Walker 1990; Pound, Bania, and Wilson 1990) reveal the existence of density peaks even in molecular clouds showing moderate extinction ( $A_V < 2 \text{ mag}$ ) on optical plates. The actual densities and sizes inferred are very uncertain because only

average values of barely resolved structures are derived from the observations. Local  $\text{H}_2$  densities in excess of a few  $10^3 \text{ cm}^{-3}$  are commonly found over scales  $l \sim 0.1 \text{ pc}$ . The CS emission observed for the high-latitude cloud MBM 12 by Pound, Bania, and Wilson implies densities larger than  $10^4 \text{ cm}^{-3}$ . These regions of enhanced density are not massive enough to be bound by self gravity: they form and dissolve over time scales related to their size and velocity dispersion by  $\tau_{\text{dyn}} \sim l/\Delta V$ . For sizes  $l \sim 0.1 \text{ pc}$  the time scale is  $\sim 3 \times 10^5 \text{ yr}$ . Density enhancements necessary for efficient condensation of molecules thus do exist even outside dense, self-gravitating concentrations of gas. At any moment only small volumes of the clouds are in a dense phase. The density enhancements are eventually torn apart by the velocity field, the matter is exposed to UV light and the photodetachment of molecules from the mantles deposited during the dense phase occurs. In addition, turbulent motions can bring pieces of clouds with different recent histories close to each other. Matter which has passed through a dense phase and for which condensation and active chemistry on grain surfaces have happened may be observed next to matter which has remained diffuse. This may provide an explanation to the variations of IR colors on small scales.

Additional complexity is introduced by the fact that the growth and composition of grain mantles does not depend only on the gas density and kinetic temperature as stated in the collision time scale in formula (1). It also depends on the relative charge of grains and molecules, which affects the sticking probability, and on the dust temperature because condensation overcomes evaporation only if dust grains are colder than some critical temperature (Léger, Jura, and Omont 1985). These physical parameters are directly coupled to the abundance of small particles which affects the penetration of UV light and consequently, the ionization balance (Lepp and Dalgarno 1988a) and dust temperature. Thus, there are several possibilities for an effective coupling between the abundance of small particles and the condensation of matter on grains. However, it is not clear if the net effect of existing couplings will be to amplify or moderate abundance inhomogeneities. Ignoring possible feedback mechanisms a simple phenomenological modeling of the scenario shows that the overall abundance of PAHs in a cloud depends on the frequency at which matter cycles between dense and diffuse phases compared with the detachment and condensation time scales.

In a cloud where matter cycles from diffuse to dense regions quickly relative to the detachment time scale no detachment will occur. In this case, if the time spent by matter in the dense phase is larger than the condensation time scale, mantles will build up on grains and few PAHs will be observed in the gas phase. In the opposite case, where density cycling is slow compared to detachment, mantles have time to be fully detached before the grains cycle through a new dense phase. Clouds with different IR colors could thus be clouds in different dynamical states, with different density structure and internal motions.

If our interpretation of the IRAS observations is correct, color variations provide a new perspective on the time scale and spatial occurrence of the cycling of interstellar matter between the gas and dust grains. To explain abundance inhomogeneities on small scales, the time scale for condensation and photoprocessing of matter on grains must be comparable to the mixing time scale of gas by turbulence. In clouds having envelopes with high  $R(12, 100)$  and  $R(25, 100)$ , the detachment of organic mantles from grains must occur on time scales

shorter or comparable to that of recycling into a dense phase. Finally, mantle formation happens not only in dark clouds of high  $A_v$ , but also in translucent clouds of smaller  $A_v$ .

#### d) Observational Tests

Although laboratory experiments on the physical processes involved in the cycling of interstellar matter on grains are too scarce to allow any quantitative modeling of the color variation along the lines proposed in this section there are several ways in which the conclusion of this work on the abundance variation of small particles and the idea raised to explain these variations can be tested. Small particles absorb mostly in the UV and have a contribution to the extinction curve which is very different from that of large dust grains. Therefore, since the variations of  $R(12, 100)$  correspond to a large change in the contribution of small particles to the absorption of starlight, an obvious way to ascertain the existence of variations in the abundance of small particles is to obtain measurements of the extinction curve toward stars located behind regions of high and low  $R(12, 100)$ .

We presently have no spectroscopic identification of the particles producing the large  $R(12, 100)$  and  $R(25, 100)$  colors at the edges of clouds. IR spectroscopy of these extended regions of low surface brightness will be feasible in the near future with the instruments on board of the Infrared Space Observatory (ISO). These observations will clarify the origin of the color variations by revealing the nature of the emitting particles. If the decrease in  $R(12, 100)$  is due to condensation of the small particles on grains,  $R(12, 100)$  should be anticorrelated with the existence of mantles. This may be tested by observations of absorption features in the IR. Detachment of small particles from dust grains is probably associated with the release of small molecules in the gas phase. The short time scale and the amount of material involved in the cycling of matter on grains are such that coupling between chemistry in the gas and on dust grains is probably more important than usually assumed. Our scenario also relates differences in IR colors and cycling of interstellar matter between gas and grain surfaces to turbulent motions in clouds. Molecular observations could thus be used to search for correlations of IR colors with the dynamical structure and chemical composition of clouds. Different means available to test the influence of grain chemistry on the chemical composition of clouds have been reviewed by Tielens and Allamandola (1987). The abundance of  $H_2O$ ,  $CH_3OH$ ,  $NH_3$ ,  $CO_2$ , and  $H_2CO$  are considered as good potential indicators of the release of molecules from grain mantles. These molecules are probably not observable in the diffuse parts of clouds, exposed to unattenuated UV radiation, where the bulk of the detachment of mantles is expected to occur. However, detachment happens at a smaller rate throughout clouds as a result of stochastic heating of grains by cosmic rays. Over a sufficiently large amount of time this slow release may build up significant and observable abundance enhancements (d'Hendecourt, Allamandola, and Greenberg 1985; d'Hendecourt *et al.* 1986).

#### VI. SUMMARY

The observations presented in this paper show that the 12 and 25  $\mu m$  emission from molecular clouds is not simply related to the 100  $\mu m$  emission and the distribution of dust as traced by  $A_v$ . In the three molecular complexes we have studied, the color ratio  $R(12, 100)$  varies across the surface of the clouds from one-quarter to five times the average value in

the solar neighborhood. The main observational properties of the variations of the  $R(12, 100)$  and  $R(25, 100)$  colors are a systematic decrease of the color with increasing  $I_v(100 \mu m)$  exemplified in many clouds by a strong limb brightening of the colors, a large scatter of colors measured for a given  $I_v(100 \mu m)$ , and the existence of large color variations both from cloud-to-cloud and on small scale within individual clouds. We show that color variations cannot be quantitatively explained by variations in the UV radiation field at the surface and within clouds. Since the existence of a source of excitation other than starlight seems unlikely in view of the high power requirements, we conclude that the color variations reflect variations in the abundance of small particles. To account for the variations in  $R(12, 100)$  the abundance of carbon in small particles in the gas phase must vary from a few percent to about one-half of the cosmic abundance. The abundance variations are likely to be related with other evidence for evolution of interstellar matter in clouds: the detection of molecular ices on grains and the observation of changes in the extinction curve (Massa and Savage 1989).

To explain the observations we propose a scenario which relates the abundance variations to a rapid cycling of interstellar matter from the gas-to-grain surfaces. In this scenario small particles form from organic mantles on grains. Regions of low  $R(12, 100)$  correspond to pieces of clouds where small particles are condensed onto grains and are not forming, while high  $R(12, 100)$  are found where small particles are detached from grain mantles by the absorption of UV photons. Within this interpretation, the overall abundance of small particles in a cloud depends on the density structure and the mixing time scale between dense and diffuse phases compared with detachment and condensation time scales. Locally within a cloud, the IR colors depend on the recent history of the matter. Where colors vary on small scales, the time scale for cycling and processing of matter on grains must be comparable to the time scale for mixing of gas by turbulent motions. IR colors and the chemical composition of the gas are predicted to be closely related to turbulent motions inside clouds. We suggest that condensation of molecules on grains occurs not only in the dense self-gravitating concentrations of molecular gas but throughout clouds in regions transiently compressed by turbulent motions. Several observations described in this paper should allow to confirm the existence of large variations in the abundance of small particles, and test the scenario proposed to explain these variations.

The research described in this paper was supported by the Centre National de Recherches Scientifiques and by the Jet Propulsion Laboratory, California Institute of Technology, under the sponsorship of the Astrophysics Division of NASA's Office of Space Science and Applications. We are grateful to Gaylin Laughlin for her help in producing the color photographs presented in the plates, and to the IPAC staff who produced the images. We thank J. P. Bernard, F. X. Désert, R. Laureijs, A. Omont, C. Rytter, and D. van Buren for fruitful discussions, and R. Harmon for a careful reading of the manuscript.

## REFERENCES

- Allamandola, L. J., Tielens, A. G. G. M., and Barker, J. R. 1987, *Interstellar Processes*, ed. D. Hollenbach and R. Thronson (Dordrecht: Reidel), p. 471.
- Allen, D. A., and Wickramasinghe, D. T. 1981, *Nature*, **294**, 239.
- Andriessse, C. D. 1978, *Astr. Ap.*, **66**, 169.
- Beichman, C., Wilson, R. W., Langer, W., and Goldsmith, P. 1988, *Ap. J. (Letters)*, **332**, L81.
- Bernard, J. P., et al. 1990, in preparation.
- Boissé, P. 1990, *Astr. Ap.*, **228**, 483.
- Boulanger, F. 1989, *The Physics and Chemistry of Interstellar Molecular Clouds*, ed. G. Winnewisser and J. T. Armstrong (Berlin: Springer), p. 30.
- Boulanger, F., Baud, B., and van Albada, G. D. 1985, *Astr. Ap.*, **144**, L9.
- Boulanger, F., Beichman, C., Désert, F. X., Helou, G., Perault, M., and Rytter, C. 1988, *Astr. Ap.*, **332**, 328.
- Boulanger, F., Bronfman, L., Koprucu, M., and Thaddeus, P. 1990, in preparation.
- Boulanger, F., Falgarone, E., Helou, G., and Puget, J. L., 1989, in *IAU Symposium 135, Interstellar Dust*, ed. L. J. Allamandola and A. G. G. M. Tielens (Washington: GPO).
- Boulanger, F., and Pérault, M. 1988, *Ap. J.*, **330**, 964.
- Butchart, I., McFadzean, A. D., Whittet, D. C. B., Geballe, T. R., and Greenberg, J. M. 1986, *Astr. Ap.*, **154**, L5.
- Cernicharo, J., Bachiller, R., and Duvert, G. 1985, *Astr. Ap.*, **149**, 273.
- Cernicharo, J., and Guélin, M. 1987, *Astr. Ap.*, **176**, 299.
- Chlewicki, G., and Laureijs, R. J. 1988, *Astr. Ap.*, **207**, L11.
- Désert, F. X., Boulanger, F., and Puget, J. L. 1990, *Astr. Ap.*, in press (DBP).
- Draine, B. T. 1985, *Protostars and Planets II*, ed. D. C. Black and M. S. Matthews (Tucson: University of Arizona Press), p. 621.
- Draine, B. T., and Anderson, N. 1985, *Ap. J.*, **292**, 494.
- Draine, B. T., and Salpeter, E. E. 1979, *Ap. J.*, **231**, 77.
- Duley, W. W. 1989, *The Physics and Chemistry of Interstellar Molecular Clouds*, ed. G. Winnewisser and J. T. Armstrong (Berlin: Springer), p. 353.
- Duvert, G., Cernicharo, J., and Baudry, A. 1986, *Astr. Ap.*, **164**, 349.
- d'Hendecourt, L. B., Allamandola, L. J., Baas, F., and Greenberg, J. M. 1982, *Astr. Ap.*, **109**, L12.
- d'Hendecourt, L. B., Allamandola, L. J., and Greenberg, J. M. 1985, *Astr. Ap.*, **152**, 130.
- d'Hendecourt, L. B., Allamandola, L. J., Grim, R. J. A., and Greenberg, J. M. 1986, *Astr. Ap.*, **158**, 119.
- d'Hendecourt, L. B., and Léger, A. 1987, *Astr. Ap.*, **180**, L9.
- de Vries, C. P., and Le Poole, R. S. 1985, *Astr. Ap.*, **145**, L7.
- de Vries, H. W., Heithausen, A., and Thaddeus, P. 1987, *Ap. J.*, **319**, 723.
- Falgarone, E., and Pérault, M. 1988, *Astr. Ap.*, **205**, L1.
- Falgarone, E., Phillips, T. G., and Walker, C. 1990, *Ap. J.*, submitted.
- Greenberg, J. M. 1982, *Submillimeter Wave Astronomy*, ed. J. E. Beckman and J. P. Phillips (Cambridge: Cambridge University Press), p. 261.
- Gregorio-Hetem, J. C., Sanzovo, G. C., and Lépine, J. R. D. 1988, *Astr. Ap. Suppl.*, **76**, 347.
- Heiles, 1984, *Ap. J. Suppl.*, **55**, 585.
- Heiles, C., Reach, W. T., and Koo, B. C. 1988, *Ap. J.*, **332**, 313.
- Helou, G. 1986, *Ap. J. (Letters)*, **311**, L33.
- Langer, W. D., Wilson, R. W., Goldsmith, P. F., and Beichman, C. 1989, *Ap. J.*, **337**, 355.
- Laureijs, R. J. 1989, Ph.D. thesis, University of Groningen.
- Laureijs, R. J., Chlewicki, G., and Clark, F. O. 1988, *Astr. Ap.*, **192**, L13.
- Laureijs, R. J., Chlewicki, G., Clark, F. O., and Wesselius, P. R. 1989, *Astr. Ap.*, **220**, 226.
- Laureijs, R. J., Mattila, K., and Schnur, G. 1987, *Astr. Ap.*, **184**, 269.
- Leene, A. 1986, *Astr. Ap.*, **154**, 295.
- Léger, A., d'Hendecourt, L. B., and Défourneau, D. 1989, *Astr. Ap.*, **216**, 148.
- Léger, A., Jura, M., and Omont, A. 1985, *Astr. Ap.*, **144**, 147.
- Léger, A., and Puget, J. L. 1984, *Astr. Ap.*, **137**, L5.
- Lepp, S., and Dalgarno, A. 1988a, *Ap. J.*, **324**, 553.
- . 1988b, *Ap. J.*, **335**, 769.
- Massa, D., and Savage, B. D. 1989, *Interstellar Dust*, ed. L. J. Allamandola and A. G. G. M. Tielens (Dordrecht: Kluwer), p. 3.
- Mathis, J. S., Ruml, W., and Nordsieck, K. H. 1977, *Ap. J.*, **217**, 425.
- Meakin, P., and Donn, B. 1988, *Ap. J. (Letters)*, **329**, L39.
- Nercessian, E., Castets, A., J. Cernicharo, J., and Benayou, J. J. 1988, *Astr. Ap.*, **189**, 207.
- Omont, A. 1986, *Astr. Ap.*, **169**, 159.
- Pérault, M., Boulanger, F., and Puget, J. L. 1990, in preparation.
- Pound, M. W., Bania, T. M., and Wilson, R. W. 1990, *Ap. J.*, **351**, 165.
- Puget, J. L. 1989, *Interstellar Dust*, ed. L. J. Allamandola and A. G. G. M. Tielens (Dordrecht: Kluwer), p. 119.
- Puget, J. L., and Léger, A., 1989, *Ann. Rev. Astr. Ap.*, **27**, 161.
- Puget, J. L., Léger, A., and Boulanger, F. 1985, *Astr. Ap.*, **142**, L19.
- Rice, W., Boulanger, F., Viallefond, F., Freedman, W., and Soifer, B. T. 1990, *Ap. J.*, **358**, 418.
- Rytter, C., Puget, J. L., and Pérault 1987, *Astr. Ap.*, **186**, 312.
- Sakata, A., and Wada, S. 1989, in *IAU Symposium 135, Interstellar Dust*, ed. L. J. Allamandola and A. G. G. M. Tielens (Washington: GPO).
- Sellgren, K., Werner, M. W., and Dinerstein, H. L. 1983, *Ap. J. (Letters)*, **271**, L13.
- Smith, R. G., Sellgren, K., and Tokunaga, A. T. 1989, *Ap. J.*, **344**, 413.
- Snell, R. L., Heyer, M. H., and Schloerb, F. P. 1989, *Ap. J.*, **337**, 739.
- Sykes, M. V. 1988, *Ap. J. (Letters)*, **334**, L55.
- Tielens, A. G. G. M., and Allamandola, L. J. 1987, *Interstellar Processes*, ed. D. Hollenbach and R. Thronson (Dordrecht: Reidel), p. 397.
- Ungerechts, H., and Thaddeus, P. 1987, *Ap. J. Suppl.*, **63**, 645.
- Verstraete, L., Léger, A., d'Hendecourt, L., Dutuit, O., and Défourneau, D. 1990, *Astr. Ap.*, submitted.
- Walterbos, R. A. M., and Schwering, P. B. W. 1987, *Astr. Ap.*, **180**, 27.
- Weikard, H., and Duvert, G. 1989, *The Physics and Chemistry of Interstellar Molecular Clouds*, ed. G. Winnewisser and J. T. Armstrong (Berlin: Springer), p. 130.
- Weiland, J. L., Blitz, L., Dwek, E., Hauser, M. G., Magnani, L., and Rickard, L. J. 1986, *Ap. J. (Letters)*, **306**, L101.
- Whittet, D. C. B., et al. 1988, *M.N.R.A.S.*, **233**, 321.

F. BOULANGER and G. HELOU: Infrared Processing and Analysis Center, 100-22, California Institute of Technology, Pasadena, CA 91125

E. FALGARONE and J. L. PUGET: Ecole Normale Supérieure, Radio-Astronomie, 24 rue Lhomond, 75005, Paris, France